

# Preparation, Characterization and Antiradical Activity of Zinc Oxide Nanoparticles

Kanyarat Kumnoedaui<sup>1</sup>, Pattareeya Damrongsak<sup>1</sup>, Kitsakorn Locharoenrat<sup>1</sup>,  
Badin Damrongsak<sup>2\*</sup>

<sup>1</sup>Biomedical Physics Research Unit, Department of Physics, Faculty of Science, King Mongkut's Institute of Technology Ladkrabang, Bangkok, 10520, Thailand

<sup>2</sup>Department of Physics, Faculty of Science, Silpakorn University, Nakornpathom, 73000, Thailand

\*Corresponding author e-mail: [badin@rocketmail.com](mailto:badin@rocketmail.com)

Received: 9 February 2022 / Revised: 27 April 2022 / Accepted: 26 May 2022

## Abstract

Zinc oxide nanoparticles (ZnO NPs) have recently been studied as a multi-functional and multi-target nanomedicine for cancer treatment. They can be used not only as a nanocarrier for delivery of the chemotherapy drug but also as an antiradical agent due to their photo-catalytic and photo-oxidizing abilities. Our previous work showed a potential use of commercial-available ZnO NPs without and with carboplatin for the treatment of retinoblastoma. The aim of this work was to synthesize ZnO NPs having smaller particle size than the commercial ones, i.e., 100 nm average diameter, in order to improve the reaction time. ZnO NPs were prepared by a sol-gel technique and calcined with different calcination conditions. The structure and particle size of ZnO powders were characterized using an x-ray diffractometer and a particle size analyzer. Average nanoparticle sizes of  $16.32 \pm 1.64$  nm were achieved at a calcination temperature of 300 degree Celsius and 1 hour holding time. The antiradical activity of prepared ZnO NPs in cooperation with ultraviolet irradiation was assessed using a putative model of cancer cells, i.e., 2,2(diphenyl-1-picrylhydrazyl) radicals (DPPH\*). An optical spectroscopy was used to detect the decrease in peak absorbance of the antiradical solution at a wavelength of 515 nm, which in turn can be used to calculate the percent remaining of DPPH\*. The disappearance of DPPH\* with respect to the reaction time revealed that prepared ZnO NPs ( $16.32 \pm 1.64$  nm) improved response time as compared with ZnO NPs (100 nm). Moreover, the effective ZnO concentrations to reduce the initial DPPH\* concentration by 50%, also known as the EC50 value in the present study, is lower indicating the improvement of anti-proliferative activity when compared to the commercial ZnO NPs.

**Keywords:** Antiradical, DPPH, Sol-gel, ZnO nanoparticles

## 1. Introduction

Zinc oxide nanoparticles (ZnO NPs) are a wide band gap semiconductor with a particle size less than 100 nm. They are one of the most abundant metal oxides, making them relatively inexpensive. ZnO NPs have, moreover, been proven non-toxic and safe to be used in food and drugs, approved by FDA (The US Food and Drug Administration). Therefore, they have received an extensive research for a long period in wide varieties of applications, from semiconductor devices (Bhati, Hojamberdiev, & Kumar, 2020; Narayana et al., 2020; Rahman, 2019; Shashanka, Esgin, Yilmaz, & Caglar, 2020) and cosmetic products (Awan et al., 2018; Nguyen, Nguyen, Le, & Le, 2020) to biomedical applications (da Silva, Caetano, Chiari-Andreo, Pietro, & Chiavacci, 2019; Martínez-Carmona, Gun'ko, & Vallet-Regi, 2018; Mishra, Mishra, Ekielski,

Talegaonkar, & Vaidya, 2017;). Currently, ZnO NPs play a significant role in modern anticancer applications (Bisht & Rayamajhi, 2016; Chen et al., 2019; Singh, Das, & Sil, 2020; Wahab et al., 2014). They not only show relatively high biocompatibility but also selective cytotoxicity against cancerous cells.

It was reported that the cytotoxicity of ZnO NPs is size-dependent. The nanoparticles with a diameter below 10 nm can penetrate more deeply in tumors and affect the cell viability; however, these small-diameter ZnO NPs can penetrate and cause toxicity to normal tissues as well. The target size for ZnO NPs is in a range of 10 – 100 nm, which is considered suitable for biomedical applications. Several methods have been studied to prepare the ZnO NPs (Devi & Velu, 2016; Manikandan, Endo, Kaneko, Murali, & John, 2018; Wallace, Brown,

Brydson, Wegner, & Milne, 2013; Wasly, Abd El-Sadek, & Henini, 2018). Among them, a chemical sol-gel process has many advantages due to ease of synthesis, cost-effectiveness and excellent homogeneity and purity. The most common precursors for synthesis of ZnO NPs are zinc acetate dihydrate, methanol and sodium hydroxide. It was reported that the size of ZnO NPs was affected by the variation in pH value of the solution (Alias, Ismail, & Mohamad, 2010). The particle size was found to decrease with an increase in the pH value.

The most widely used method for evaluating the antiradical properties of ZnO NPs is by scavenging free radicals of 2,2-diphenyl-1-picrylhydrazyl hydrate (DPPH\*) with varying the concentration of the nanoparticles (Brand-Williams, Cuvelier, & Berset, 1995). UV-visible spectrometry is typically employed to measure the absorbance of the mixtures as the indirect measurement of the antiradical activity.

In our previous study (Pairoj et al., 2019), the antiradical performance of commercial ZnO NPs was investigated for being used as an anticancer drug for retinoblastoma treatment. The results showed that the nanoparticles alone had low antiradical efficiency and the number of reduced DPPH\* increased by applying UV illumination. In this work, we aimed to prepare ZnO NPs with a diameter less than 100 nm (the size of the commercially available ZnO NPs) in order to improve the antiradical activity. The sol-gel method was chosen to synthesize ZnO NPs. The synthesized NPs were characterized and compared with those results obtained from the commercially available nanoparticles.

## 2. Materials and Methods

### 2.1 Materials

Precursors used for the formation of the zinc oxide nanoparticles were zinc acetate dihydrate ( $\text{Zn}(\text{CH}_3\text{COO})_2 \cdot 2\text{H}_2\text{O}$ ) with  $\geq 99.5\%$  purity and sodium hydroxide (NaOH) with  $\geq 97\%$  purity. Both were purchased from KemAus. Sodium hydroxide was used to control the pH of the solution. Methanol ( $> 99.9\%$ , from Labsupplies) was used as a reagent and DI water was used for dilution.

### 2.2 Methods

#### (1) Synthesis of ZnO NPs

The ZnO sols were prepared by adding 0.15 M ( $\text{Zn}(\text{CH}_3\text{COO})_2 \cdot 2\text{H}_2\text{O}$ ) to methanol at room temperature. The solution was stirred at a temperature of 70°C for 90 min using a magnetic stirrer until a clear solution without turbidity was obtained. The pH level of the solution affects the particle size of synthesized ZnO powders (Alias et al., 2010; Rani, Suri, Shishodia, & Mehra, 2008). Therefore, the prepared solution was adjusted to the pH value of 10 by adding 1.5 M NaOH, aiming to control the size of ZnO particles close to 10 nm. The resulting milky white gel was then stirred at a temperature of 70°C for 60 minutes. After this process, the sol was centrifuged for 15 minutes at 5000 rpm. The sample was washed with a 40:60 mixture of DI water and ethanol in order to remove organic materials left on the surface of synthesized ZnO powders. The sediment was dried at 100°C for 8 hours. Finally, the dried precipitate was calcined in air at 300°C for 60 minutes.

#### (2) Physical characterization

The crystal structure of the synthesized samples was determined by the Rigaku X-ray diffractometer (XRD). The X-ray source of Cu K $\alpha$  radiation, having the monochromatic wavelength of 1.5406 Å, was used. The diffraction pattern was recorded in the range of 20-80° for the ZnO samples. The XRD results were compared to the Joint Committee on Powder Diffraction Standards (JCPDS) data file. The crystallite size of the samples was estimated using the Scherrer formula:

$$d_{XRD} = \frac{K\lambda}{B \cos \theta} \quad (1)$$

where  $d_{XRD}$  is the average diameter of nanoparticles, K is a shape factor (0.9 for spherical particles),  $\lambda$  is the wavelength of X-ray source (1.5406 Å), B is the line broadening of the strong XRD peak (101) at half its peak height, and  $\theta$  is the Bragg angle.

#### (3) Determination of antiradical activity

The antiradical activity of the prepared ZnO NPs was determined by a spectrophotometric method, also called DPPH method. In this method, a solution of 2,2-diphenyl-1-picrylhydrazyl (DPPH\*) was used as the putative model of cancer cells (Aruoma & Cuppett, 1997), acting as a free radical source. Prior adding a solution of synthesized ZnO NPs into the solution, the DPPH\* the solution had a deep violet color. When a solution of synthesized ZnO NPs was added into the DPPH\* solution, the

free radicals were scavenged resulting in a change of the color in the solution as shown in Figure 1. This process was quantitatively monitored by measuring the absorbance spectra of the solution using Avantes UV-visible spectrometer.

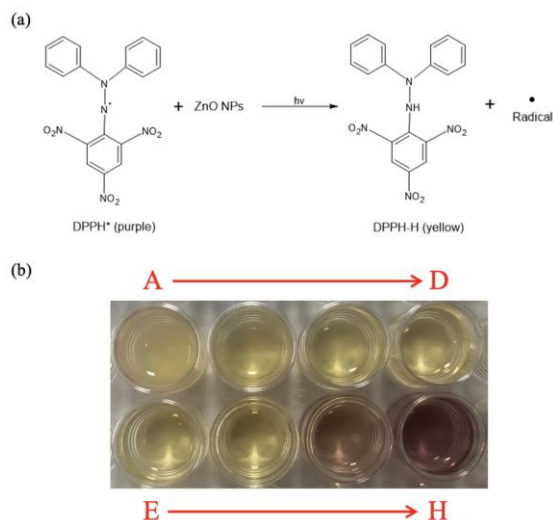


**Figure 1.** (a) Mechanism of the DPPH\* scavenging activity of the ZnO NPs. (Marin-Flores et al., 2021) (b) The color change of DPPH\* with respect to the different concentrations of ZnO NPs at 1440 min. A, B, C, D, E, F, G, and H represent 1.000, 0.500, 0.250, 0.125, 0.0625, 0.03125, 0.0156, and 0.0078 mg/ml respectively.

In this experiment, a 100  $\mu$ M solution of the DPPH\* Methanol was prepared and then added with a solution of the synthesized nanoparticles at various concentrations, ranging from 0.0078 to 1.000 mg/ml. The mixture was sonicated for 90 minutes at room temperature. Each mixed solution was illuminated by an 8 W, 254 nm UV lamp (Spectroline: CX-21, Germany) in order to introduce the photoexcitation process. After that, the solution was taken for measuring the absorbance at a peak wavelength of 515 nm for a time duration from 0 to 1440 minutes (no decrease in the absorbance can be observed). The percentage of residual DPPH\* with respect to the reaction time was calculated using:

$$\%RemainingDPPH^* = \frac{C_{ss}}{C_{is}} \times 100 \quad (2)$$

where  $C_{is}$  and  $C_{ss}$  are to concentration of DPPH\* at initial state and steady state, respectively. The

concentrations of DPPH\* were determined by using the linear equation obtained from the calibration curve reported in Pairoj et al., 2019.

$$C_{DPPH^*} = (Abs_{515nm} - 0.0132)/0.0072 \quad (3)$$

### 3. Results and Discussion

The X-ray diffraction pattern of prepared ZnO NPs was shown in Figure 2. It showed the diffraction peaks at angles of 31.78°, 33.9°, 36.8°, 47.63°, 56.67°, 62.94° and 67.98°, respectively, corresponding to the Bragg reflections (100), (002), (101), (102), (110), (103) and (112) of ZnO having a typical hexagonal wurtzite structure. All peaks were in good agreement with the standard JCPDS file no. 01-084-6784 (Kinnunen, Lahtinen, Arstila, & Sajavaara, 2021). From Scherrer formula, the average crystalline size of the prepared ZnO NPs was  $16.32 \pm 1.64$  nm. The size of the synthesized nanoparticles was approximately 5 times smaller than that of commercial ZnO NPs (Sigma Aldrich, USA having a diameter of 100 nm) which was used as a reference.

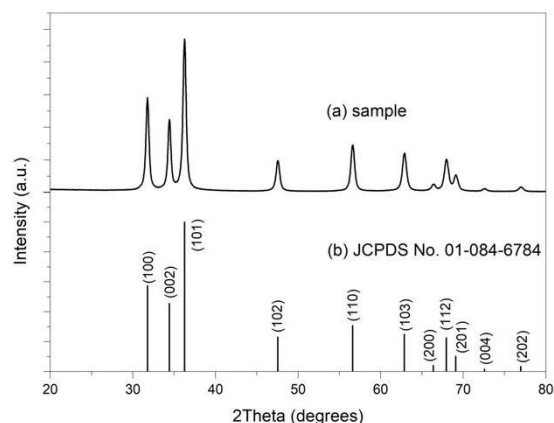


**Figure 2.** XRD pattern of the synthesized ZnO NPs.

The antiradical activity of prepared ZnO NPs was measured by monitoring the color of the DPPH\* solution after adding the ZnO NPs for some period of time until the reaction reaches a steady state. The solution was illuminated by a constant power UV light source at a room temperature. At every 10 minutes, one tube of the samples was taken out in order to measure the absorbance spectrum. Figure 3

shows an example of the monitored absorbance spectra for the DPPH\* solution in the presence of ZnO NPs with the concentration of 0.25 mg/ml. It can be observed that a peak intensity at 515 nm moderately decreases with time and starts reaching a steady state after 250 minutes. A decrease of the peak absorbance is related to a change in color of the solution, which can be implied that the added ZnO NPs scavenged the free radicals in the DPPH\* solution over time. The peak absorbance values at the wavelength of 515 nm were recorded to determine the antiradical activity of the tested ZnO NPs.

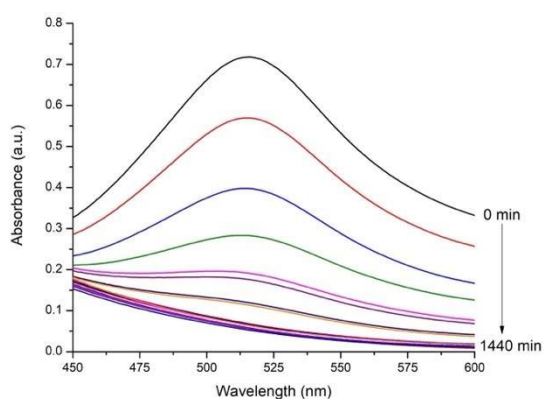
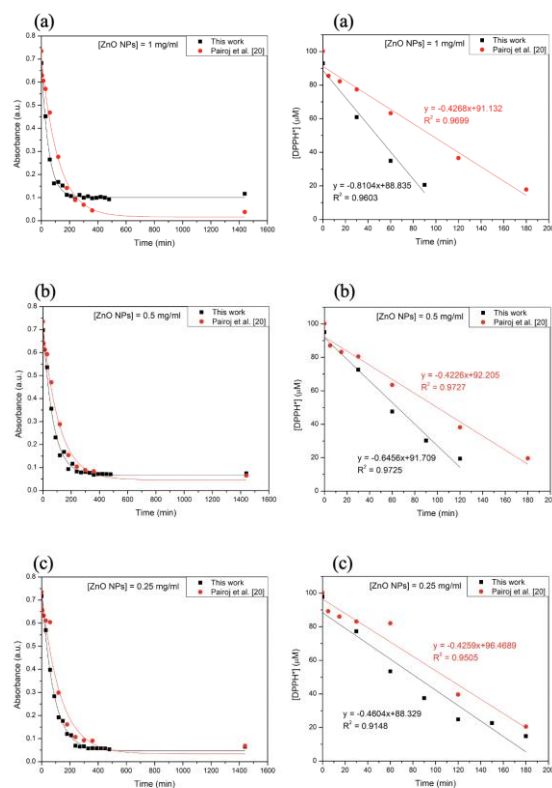


**Figure 3.** Absorbance spectra for the DPPH\* solution in the presence of ZnO NPs with the concentration of 0.25 mg/ml at a different time interval.

The peak absorbance at 515 nm as a function of exposed time for the prepared ZnO NPs with different concentrations was plotted and compared with those obtained from the reference commercial ZnO NPs. For a quantitative comparison, the DPPH\* concentration that calculated from equation (3) was plotted against the exposed time in order to estimate the rate of reaction (Rs). For a sake of clarity, only the linear region was considered. The rate of reaction at which the DPPH\* concentration decreased over the exposed time can then be estimated from the slope. Figure 4 shows the peak absorbance of the DPPH\* solution and DPPH\* concentration in the presence of ZnO NPs. The rate of reaction corresponding to the concentration of the synthesized and the reference ZnO NPs was shown in Figure 5. As can be seen, the rate of reaction increases when the nanoparticle concentration increases, having a similar trend for both the ZnO

NPs prepared in this work and the commercial ones. The rate of reaction obtained from the nanoparticles in this work, which have much smaller particle size (16 nm), was slightly higher. Interestingly, it was observed that the rate of reaction of the commercial ZnO NPs reached the saturation state when the solution concentration was over 0.25 mg/ml. On the other hand, the smaller size of the prepared ZnO NPs still kept attacking the free radicals even though the concentration was as high as 1 mg/ml.

To summarize, the ability of the free radical scavenging activity of the prepared ZnO NPs was better than the reference nanoparticles. This was due to the relatively smaller size of the prepared nanoparticles, making them be able to penetrate more deeply in the putative model or in our case the DPPH\*. In addition, the smaller size leads to a high surface area to volume ratio, which in turn increases a surface contact to the targeted radicals. In addition, under UV irradiation, the prepared nanoparticles were able to release much more amount of toxic Zn<sup>2+</sup> ions into the DPPH\* due to the large surface area.



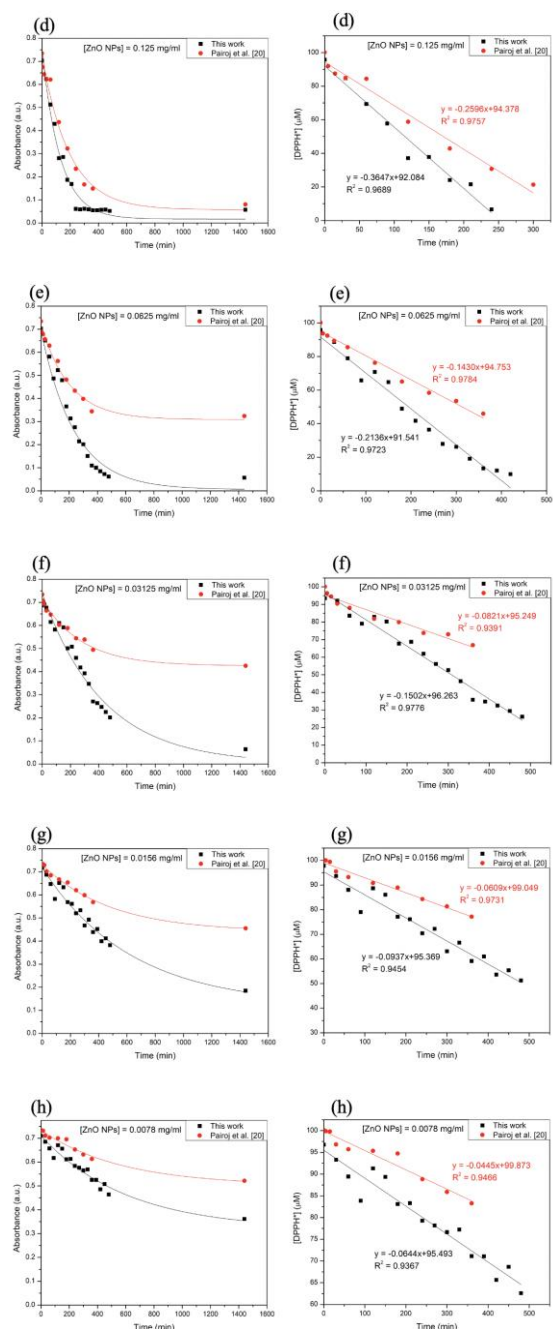


**Figure 4.** Peak absorbance at 515 nm and DPPH\* concentration corresponding to the exposed time for the DPPH\* solution in the presence of ZnO NPs with the concentration of (a) 1.000 mg/ml, (b) 0.500 mg/ml, (c) 0.250 mg/ml, (d) 0.125 mg/ml, (e) 0.0625 mg/ml, (f) 0.03125 mg/ml, (g) 0.0156 mg/ml, and (h) 0.0078 mg/ml.

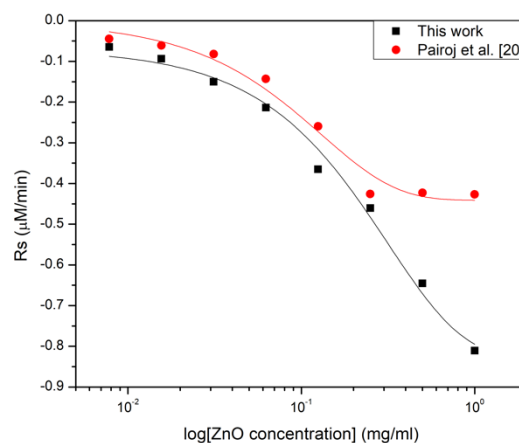


**Figure 5.** Rate of reaction (Rs) corresponding to the concentrations of ZnO NPs; a black line represents the data from the prepared ZnO NPs in this work, while a red line represents the data obtained from the reference commercial ZnO NPs.

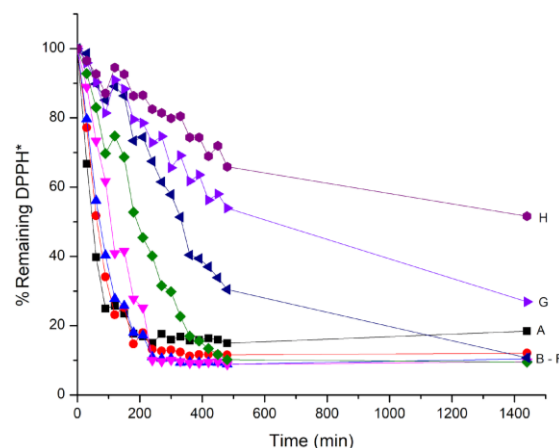


**Figure 6.** The percentage of residual DPPH\* with respect to the reaction time at the different concentration. A, B, C, D, E, F, G, and H represent 1.000, 0.500, 0.250, 0.125, 0.0625, 0.03125, 0.0156, and 0.0078 mg/ml respectively.

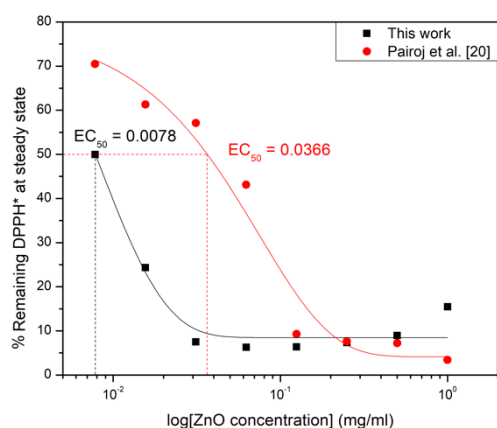


**Figure 7.** The percentage of residual DPPH\* with respect to a mole ratio of antiradical agent to DPPH\*. The effective concentration (EC<sub>50</sub>) value of each antiradical agent is also presented.

In biological studies, a half maximal effective concentration (EC<sub>50</sub>), which is defined as the concentration of ZnO NPs sample required for a 50% decrease in the DPPH\* concentration, is typically used to express and compare the efficiency of the antiradical activity with different other samples. Thus, the amount of residual DPPH\* in the presence of the prepared ZnO NPs at different concentrations was calculated using equations (2) and the percent remaining of the DPPH\* corresponding to the reaction time was shown in Figure 6. In Figure 7, The percentage of residual DPPH\* at a steady state (1440 minutes of the reaction) with regard to the concentration of ZnO NPs was plotted in order to estimate the EC<sub>50</sub> value. As can be seen, the EC<sub>50</sub> value in this work was approximately 5 times lower than the EC<sub>50</sub> obtained from the commercial ZnO NPs. This can be implied that the antiradical activity had significantly improved.

#### 4. Conclusions

ZnO NPs were synthesized by using a sol-gel method. By adjusting the pH of the solution, ZnO NPs with an average particle size of  $16.32 \pm 1.64$  nm were achieved. The free radical scavenging capacity of the ZnO NPs at different concentrations was analyzed using the DPPH test; in this study, the rate of reaction and EC<sub>50</sub> value were determined and compared with results obtained from the commercial ZnO NPs used in our previous work. According to the experimental results, the ability of the free

radical scavenging activity of the prepared ZnO NPs was significantly improved over the reference nanoparticles. The EC<sub>50</sub> value of the ZnO NPs in this work was approximately 5 times better than the results from the commercial ZnO NPs (100 nm in diameter). This was obvious that the relatively smaller size of the prepared ZnO NPs made them penetrating deeper into the DPPH\*. Because of the large surface area, the particles had more chance to contact the targeted radicals and, under the UV photoexcitation, were able to produce many toxic Zn<sup>2+</sup> ions, increasing the antiradical activity.

#### 5. Acknowledgement

Authors would like to thank the National Research Council of Thailand (NRCT), Silpakorn University and King Mongkut's Institute of Technology Ladkrabang for financial support.

#### 6. References

- Alias, S. S., Ismail, A. B., & Mohamad, A. A. (2010). Effect of pH on ZnO nanoparticle properties synthesized by sol-gel centrifugation. *Journal of Alloys and Compounds*, 499(2), 231-237. doi:10.1016/j.jallcom.2010.03.174
- Aruoma, O. I., & Cuppett, S. L. (Eds.). (1997). *Antioxidant methodology: In vivo and in vitro concepts*. The American Oil Chemists Society.
- Awan, F., Islam, M. S., Ma, Y., Yang, C., Shi, Z., Berry, R. M., & Tam, K. C. (2018). Cellulose nanocrystal-ZnO nanohybrids for controlling photocatalytic activity and UV protection in cosmetic formulation. *ACS Omega*, 3(10), 12403-12411. doi:10.1021/acsomega.8b01881
- Bhati, V. S., Hojamberdiev, M., & Kumar, M. (2020). Enhanced sensing performance of ZnO nanostructures-based gas sensors: A review. *Energy Reports*, 6, 46-62. doi:10.1016/j.egy.2019.08.070
- Bisht, G., & Rayamajhi, S. (2016). ZnO nanoparticles: A promising anticancer agent. *Nanobiomedicine*, 3. doi:10.5772/63437
- Brand-Williams, W., Cuvelier, M. E., & Berset, C. (1995). Use of a free radical method to evaluate antioxidant activity. *LWT-Food Science and Technology*, 28(1), 25-30. doi:10.1016/S0023-6438(95)80008-5
- Chen, P., Wang, H., He, M., Chen, B., Yang, B., & Hu, B. (2019). Size-dependent cytotoxicity study of ZnO nanoparticles in HepG2

- cells. *Ecotoxicology and Environmental Safety*, 171, 337-346.  
doi:10.1016/j.ecoenv.2018.12.096
- da Silva, B. L., Caetano, B. L., Chiari-Andréo, B. G., Pietro, R. C. L. R., & Chiavacci, L. A. (2019). Increased antibacterial activity of ZnO nanoparticles: Influence of size and surface modification. *Colloids and Surfaces B: Biointerfaces*, 177, 440-447.  
doi:10.1016/j.colsurfb.2019.02.013
- Devi, P. G., & Velu, A. S. (2016). Synthesis, structural and optical properties of pure ZnO and Co doped ZnO nanoparticles prepared by the co-precipitation method. *Journal of Theoretical and Applied Physics*, 10(3), 233-240. doi:10.1007/s40094-016-0221-0
- Kinnunen, S., Lahtinen, M., Arstila, K., & Sajavaara, T. (2021). Hydrogen and deuterium incorporation in ZnO films grown by atomic layer deposition. *Coatings*, 11(5), 542.  
doi:10.3390/coatings11050542
- Manikandan, B., Endo, T., Kaneko, S., Murali, K. R., & John, R. (2018). Properties of sol gel synthesized ZnO nanoparticles. *Journal of Materials Science: Materials in Electronics*, 29(11), 9474-9485.  
doi:10.1007/s10854-018-8981-8
- Marin-Flores, C. A., Rodríguez-Nava, O., García-Hernández, M., Ruiz-Guerrero, R., Juárez-López, F., & Morales-Ramírez, A. D. J. (2021). Free-radical scavenging activity properties of ZnO sub-micron particles: Size effect and kinetics. *Journal of Materials Research and Technology*, 13, 1665-1675.  
doi:10.1016/j.jmrt.2021.05.050
- Martínez-Carmona, M., Gun'ko, Y., & Vallet-Regí, M. (2018). ZnO nanostructures for drug delivery and theranostic applications. *Nanomaterials*, 8(4), 268.  
doi:10.3390/nano8040268
- Mishra, P. K., Mishra, H., Ekielski, A., Talegaonkar, S., & Vaidya, B. (2017). Zinc oxide nanoparticles: A promising nanomaterial for biomedical applications. *Drug Discovery Today*, 22(12), 1825-1834.  
doi:10.1016/j.drudis.2017.08.006
- Narayana, A., Bhat, S. A., Fathima, A., Lokesh, S. V., Surya, S. G., & Yelamaggad, C. V. (2020). Green and low-cost synthesis of zinc oxide nanoparticles and their application in transistor-based carbon monoxide sensing. *RSC Advances*, 10(23), 13532-13542.  
doi:10.1039/D0RA00478B
- Nguyen, N. T., Nguyen, T. M. N., Le, N. T., & Le, T. K. (2020). Suppressing the photocatalytic activity of ZnO nanoparticles by Al-doping for the application in sunscreen products. *Materials Technology*, 35(6), 349-355. doi:10.1080/10667857.2019.1684733
- Pairaj, S., Damrongsak, P., Damrongsak, B., Jinawath, N., Kaewkhaw, R., Leelawattananon, T., ... & Locharoenrat, K. (2019). Antiradical properties of chemo drug, carboplatin, in cooperation with ZnO nanoparticles under UV irradiation in putative model of cancer cells. *Biocybernetics and Biomedical Engineering*, 39(3), 893-901.  
doi:10.1016/j.bbe.2019.08.004
- Rahman, F. (2019). Zinc oxide light-emitting diodes: A review. *Optical Engineering*, 58(1).  
doi:10.1117/1.OE.58.1.010901
- Rani, S., Suri, P., Shishodia, P. K., & Mehra, R. M. (2008). Synthesis of nanocrystalline ZnO powder via sol-gel route for dye-sensitized solar cells. *Solar Energy Materials and Solar Cells*, 92(12), 1639-1645.  
doi:10.1016/j.solmat.2008.07.015
- Shashanka, R., Esgin, H., Yilmaz, V. M., & Caglar, Y. (2020). Fabrication and characterization of green synthesized ZnO nanoparticle based dye-sensitized solar cells. *Journal of Science: Advanced Materials and Devices*, 5(2), 185-191. doi:10.1016/j.jsamd.2020.04.005
- Singh, T. A., Das, J., & Sil, P. C. (2020). Zinc oxide nanoparticles: A comprehensive review on its synthesis, anticancer and drug delivery applications as well as health risks. *Advances in Colloid and Interface Science*, 286.  
doi:10.1016/j.cis.2020.102317
- Wahab, R., Siddiqui, M. A., Saquib, Q., Dwivedi, S., Ahmad, J., Musarrat, J., ... Shin, H. S. (2014). ZnO nanoparticles induced oxidative stress and apoptosis in HepG2 and MCF-7 cancer cells and their antibacterial activity. *Colloids and Surfaces B: Biointerfaces*, 117, 267-276.  
doi:10.1016/j.colsurfb.2014.02.038
- Wallace, R., Brown, A. P., Brydson, R., Wegner, K., & Milne, S. J. (2013). Synthesis of ZnO nanoparticles by flame spray pyrolysis and characterisation protocol. *Journal of Materials Science*, 48(18), 6393-6403.  
doi:10.1007/s10853-013-7439-x
- Wasly, H. S., Abd El-Sadek, M. S., & Henini, M. (2018). Influence of reaction time and synthesis temperature on the physical properties of ZnO nanoparticles synthesized by the hydrothermal method. *Applied Physics A*, 124, 1-12. doi:10.1007/s00339-017-1482-4